筑波大学
University of Tsukuba

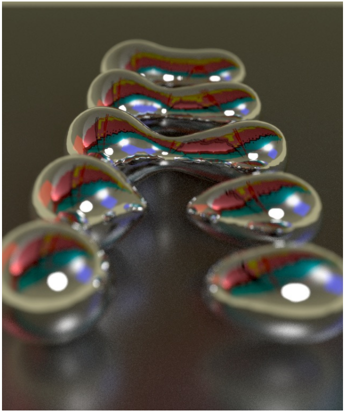

Center for Computational Sciences

December 10-12, 2018

CCS workshop

Impact of pear-shaped fission fragments on mass-asymmetric fission

Guillaume SCAMPS

Collaboration : C. Simenel

Motivation : understand the shell effects on fission

Empirical behavior of actinide nuclei

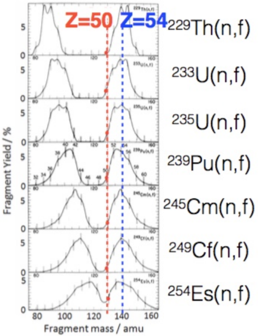

J.P. Unik, J.E. Gindler, J.E. Glendenin et al. : Proc. Phys. and Chem. of Fission IAEA Vienna , Vol II, 20 (1974)

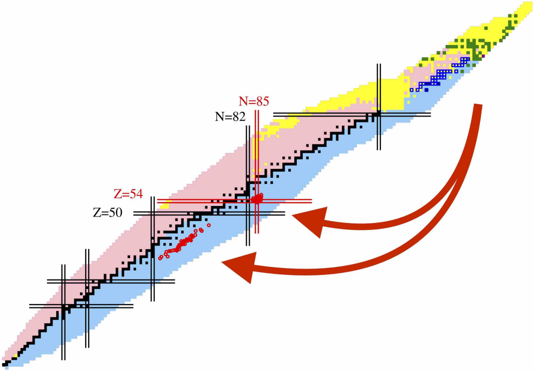

Data from D. A. Brown et al., Endf/b-viii.0, Nucl. Data Sheets 148, 1 (2018), (spontaneous and thermal neutron-capture).

Systematic comparison for actinide

Empirical behavior of actinide nuclei

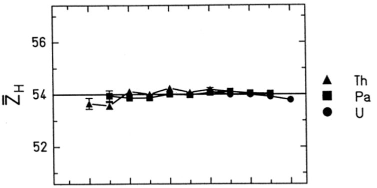

K.-H. Schmidt et al. Nuclear Physics A 665 (2000)

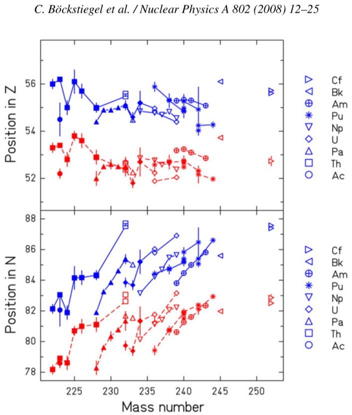

Motivation

How can we understand this behavior ? Interplay between structure and reaction ?

Mean-field theory with pairing

TDHF

- Independent particle
- Initialisation : $\hat{h}_{MF} \left|\phi_i\right\rangle = \epsilon_i \left|\phi_i\right\rangle$
- Evolution :
  $i\hbar \frac{d\rho}{dt} = [h_{MF}, \rho]$

TDHFB

- Pairing correlation
- Quasi-particles : $\left|\omega_\alpha\right\rangle = \begin{pmatrix} U_\alpha \\ V_\alpha \end{pmatrix}$
- Evolution :
  $i\hbar \frac{d\left|\omega_\alpha\right\rangle}{dt} = \begin{pmatrix} h & \Delta \\ -\Delta^* & -h^* \end{pmatrix} \left|\omega_\alpha\right\rangle$

TDHF+BCS

- Based on TDHFB with the approximation : $\Delta_{ij} = \delta_{ij}\Delta_i$
- Evolution : $i\hbar \frac{d\phi_i}{dt} = (\hat{h}_{MF} - \epsilon_i)\phi_i$
  $i\hbar \frac{dn_i}{dt} = \Delta_i^* \kappa_i - \Delta_i \kappa_i^*$
  $i\hbar \frac{d\kappa_i}{dt} = \kappa_i(\epsilon_i - \epsilon_{\bar{i}}) + \Delta_i(2n_i - 1)$

Why does we need pairing ?

Fission barrier : ^{258}Fm

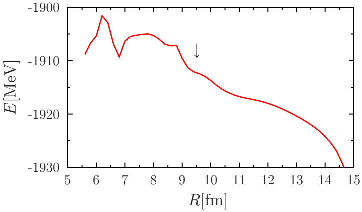

TDHF

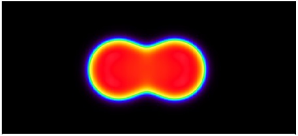

TDHF+BCS

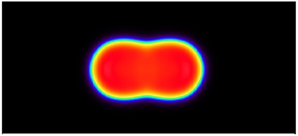

G. Scamps, C. Simenel, D. Lacroix, PRC **92**, 011602(R) (2015).

Why does we need pairing ?

Fission barrier : ^{258}Fm

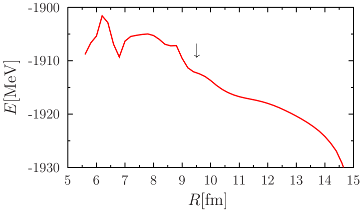

TDHF

TDHF+BCS

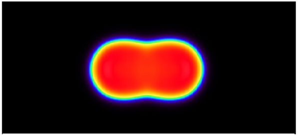

G. Scamps, C. Simenel, D. Lacroix, PRC **92**, 011602(R) (2015).

Why does we need pairing ?

Fission barrier : ^{258}Fm

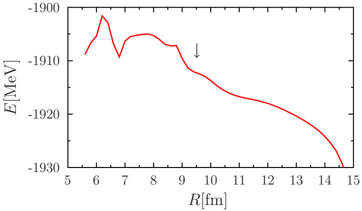

TDHF

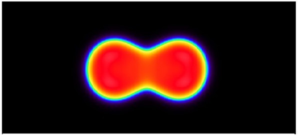

TDHF+BCS

G. Scamps, C. Simenel, D. Lacroix, PRC **92**, 011602(R) (2015).

Influence of pairing on fission process

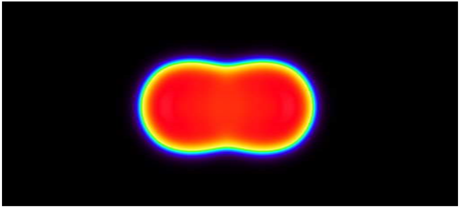

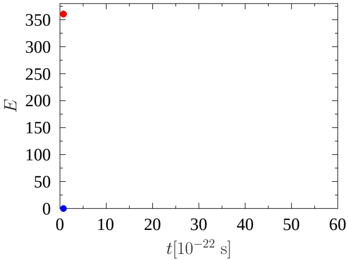

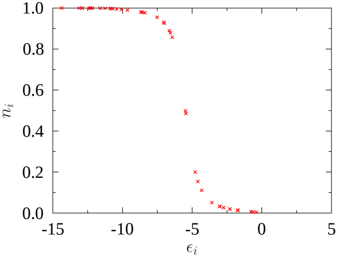

Influence of pairing on fission process

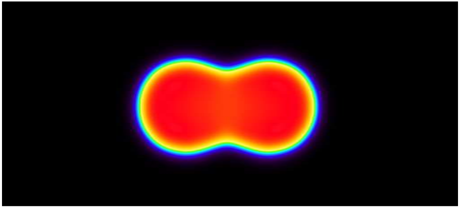

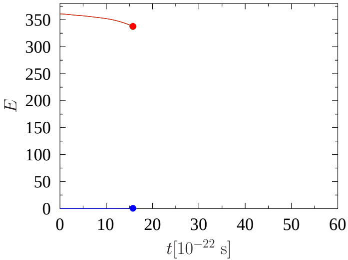

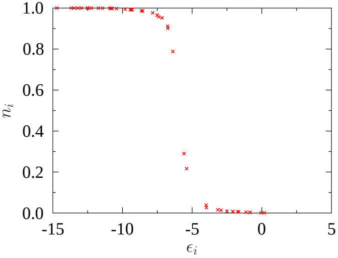

Influence of pairing on fission process

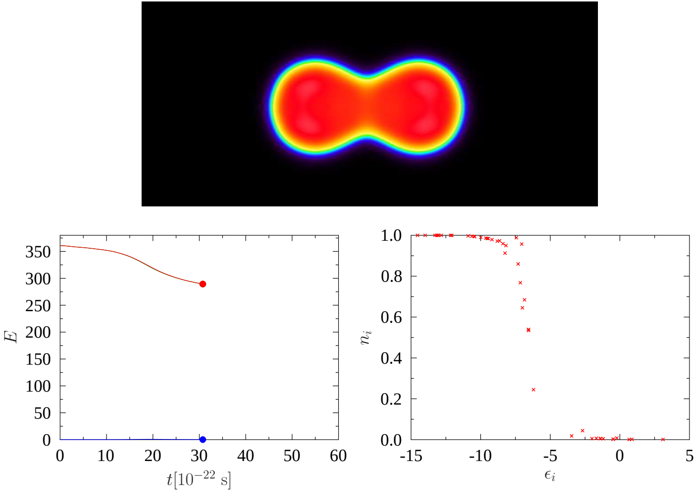

Influence of pairing on fission process

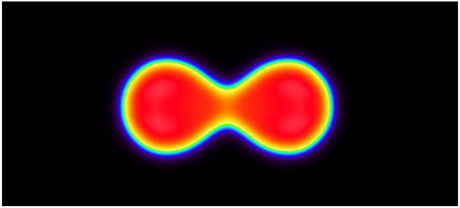

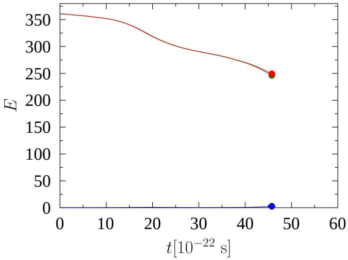

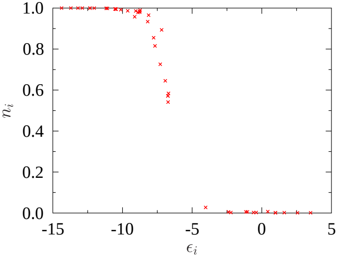

Influence of pairing on fission process

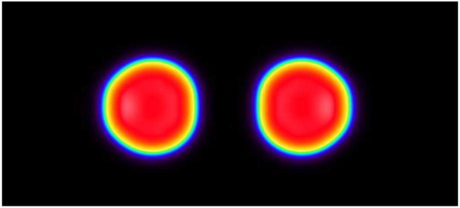

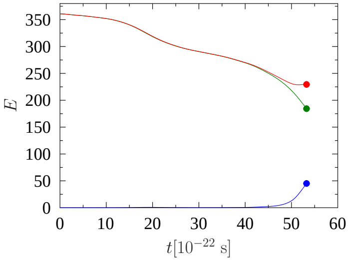

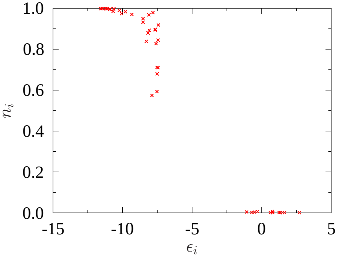

New systematic study

First : CHF+BCS

Example : ^{240}Pu

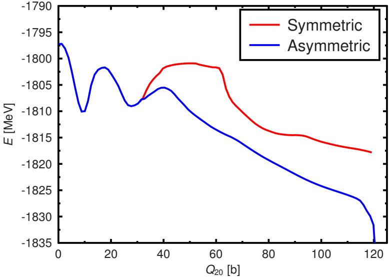

Second : TDHF+BCS

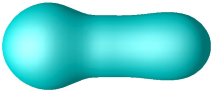

Details of the calculation

- Skyrme functionnal Sly4d
- Surface pairing interaction
- $\Delta x = 0.8$ fm
- Lattice : $L \times L \times 2L = 40 \times 19.2 \times 19.2$ fm^3

New systematic study

First : CHF+BCS

Example : ^{240}Pu

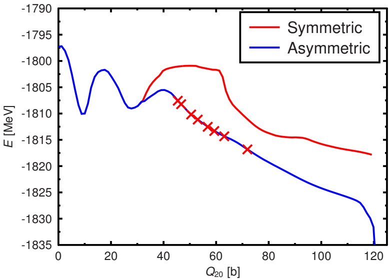

Second : TDHF+BCS

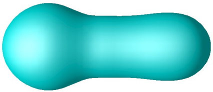

Details of the calculation

- Skyrme functionnal Sly4d
- Surface pairing interaction
- $\Delta x = 0.8$ fm
- Lattice : $L_x \times L_y \times 2L_z = 40 \times 19.2 \times 19.2$ fm^3

New systematic study

First : CHF+BCS

Example : ^{240}Pu

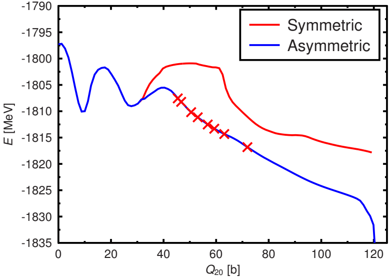

Second : TDHF+BCS

Details of the calculation

- Skyrme functionnal Sly4d
- Surface pairing interaction
- $\Delta x = 0.8$ fm
- Lattice : $L_x \times L_y \times 2L_z = 40 \times 19.2 \times 19.2$ fm^3

TDHF+BCS systematics results

TDHF+BCS

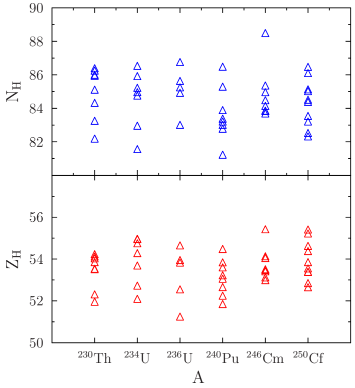

Comparison with experimental data

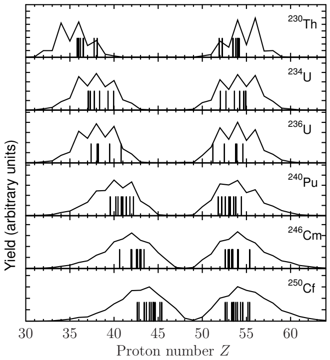

TDHF+BCS systematics results

TDHF+BCS

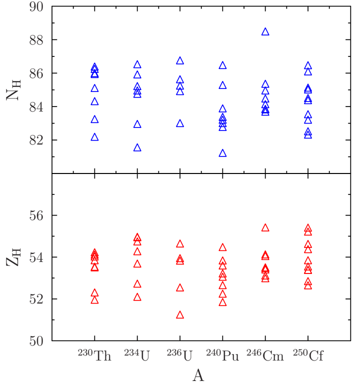

Comparison with experimental data

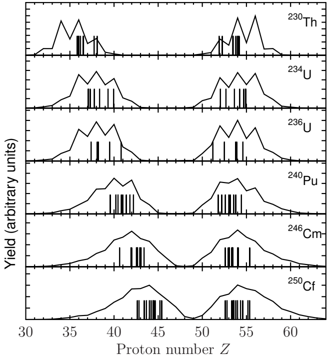

Conclusion :

The TDHF+BCS calculation reproduces well the Z=54 behavior. But why ?

Nucleon localization function

Fermion localization function

$$\mathcal{C}_{q\sigma}(\mathbf{r}) = \left[1 + \left(\frac{\tau_{q\sigma}\rho_{q\sigma} - \frac{1}{4}|\nabla\rho_{q\sigma}|^2 - \mathbf{j}^2_{q\sigma}}{\rho_{q\sigma}\tau^{TF}_{q\sigma}}\right)^2\right]^{-1}$$

A. D. Becke and K. E. Edgecombe, J. Chem. Phys. 92, 5397 (1990).

Physical meaning :
$\mathcal{C} \in [0:1]$
$\mathcal{C}_{q\sigma}(\mathbf{r}) = 1$ Probability to find another particle with the same q and σ very low.
$\mathcal{C}_{q\sigma}(\mathbf{r}) = 0.5$ Limit of uniform-density Fermi gas.

Mask function :

$$\rightarrow \frac{\mathcal{C}_{q\sigma}(\mathbf{r})\rho_{q\sigma}}{\rho^{\max}_{q\sigma}}$$

Nucleon localization function

Fermion localization function

$$\mathcal{C}_{q\sigma}(\mathbf{r}) = \left[1 + \left(\frac{\tau_{q\sigma}\rho_{q\sigma} - \frac{1}{4}|\nabla\rho_{q\sigma}|^2 - \mathbf{j}^2_{q\sigma}}{\rho_{q\sigma}\tau^{TF}_{q\sigma}}\right)^2\right]^{-1}$$

A. D. Becke and K. E. Edgecombe, J. Chem. Phys. 92, 5397 (1990).

Physical meaning :
$\mathcal{C} \in [0:1]$
$\mathcal{C}_{q\sigma}(\mathbf{r}) = 1$ Probability to find another particle with the same q and σ very low.
$\mathcal{C}_{q\sigma}(\mathbf{r}) = 0.5$ Limit of uniform-density Fermi gas.

Mask function :

$$\rightarrow \frac{\mathcal{C}_{q\sigma}(\mathbf{r})\rho_{q\sigma}}{\rho^{\max}_{q\sigma}}$$

Example :

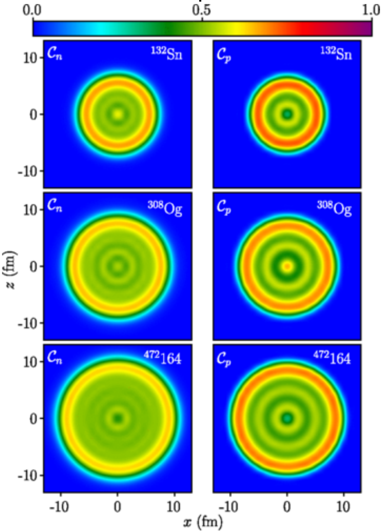

P. Jerabek, B. Schuetrumpf, P. Schwerdtfeger, and W. Nazarewicz, Phys. Rev. Lett. **120**, 053001 (2018).

Nucleon localization function

Fermion localization function

$$\mathcal{C}_{q\sigma}(\mathbf{r}) = \left[1 + \left(\frac{\tau_{q\sigma}\rho_{q\sigma} - \frac{1}{4}|\nabla\rho_{q\sigma}|^2 - \mathbf{j}^2_{q\sigma}}{\rho_{q\sigma}\tau^{TF}_{q\sigma}}\right)^2\right]^{-1}$$

A. D. Becke and K. E. Edgecombe, J. Chem. Phys. 92, 5397 (1990).

Physical meaning :
$\mathcal{C} \in [0:1]$
$\mathcal{C}_{q\sigma}(\mathbf{r}) = 1$ Probability to find another particle with the same q and σ very low.
$\mathcal{C}_{q\sigma}(\mathbf{r}) = 0.5$ Limit of uniform-density Fermi gas.

Mask function :

$$\rightarrow \frac{\mathcal{C}_{q\sigma}(\mathbf{r})\rho_{q\sigma}}{\rho^{\max}_{q\sigma}}$$

Schematic system

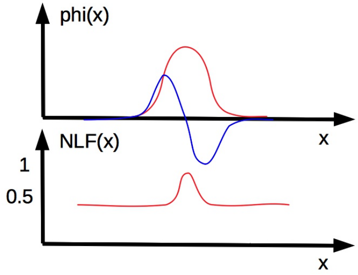

Example of ^{240}Pu

^{240}Pu

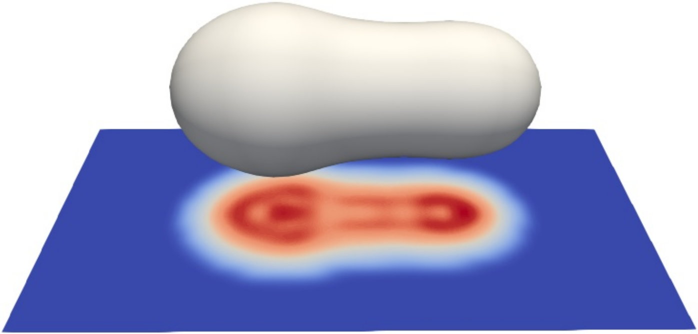

Example of ^{240}Pu

^{240}Pu

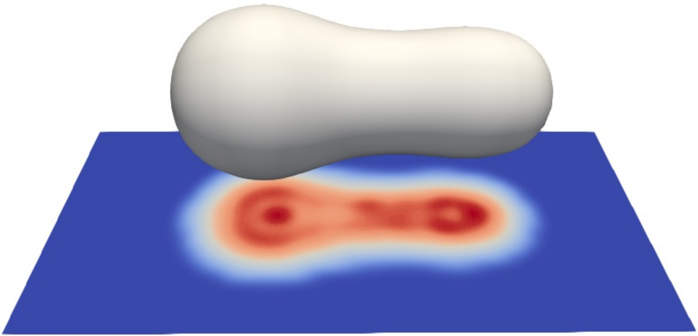

Example of ^{240}Pu

^{240}Pu

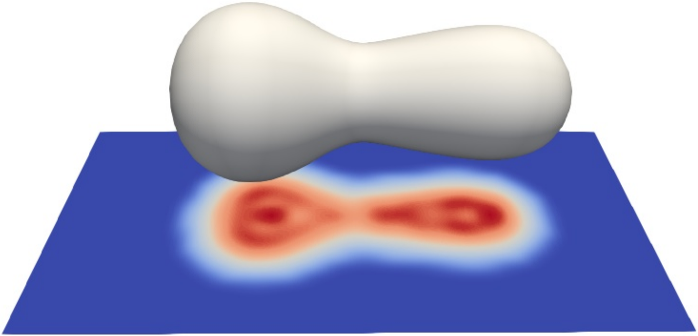

Example of ^{240}Pu

^{240}Pu

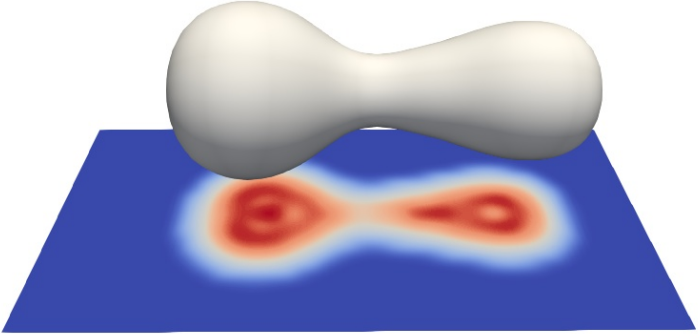

Example of ^{240}Pu

^{240}Pu

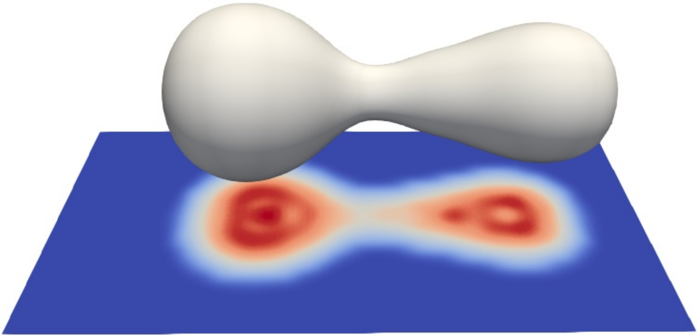

Example of ^{240}Pu

^{240}Pu

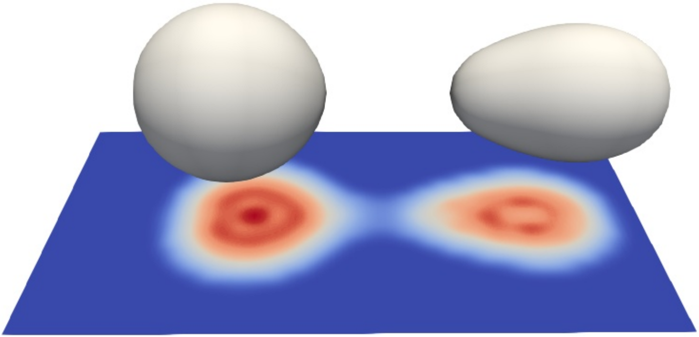

Example of ^{240}Pu

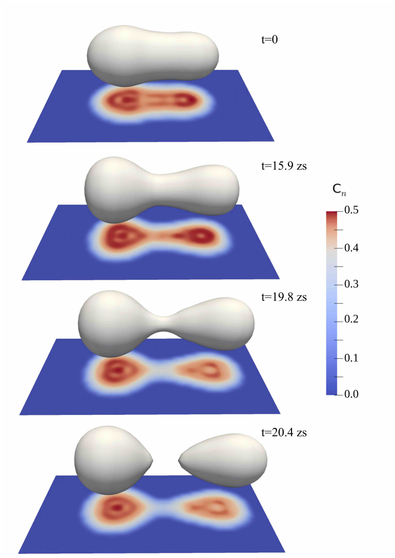

Hypothesis

The octupole shell effects are important in the fission fragment

Other systems

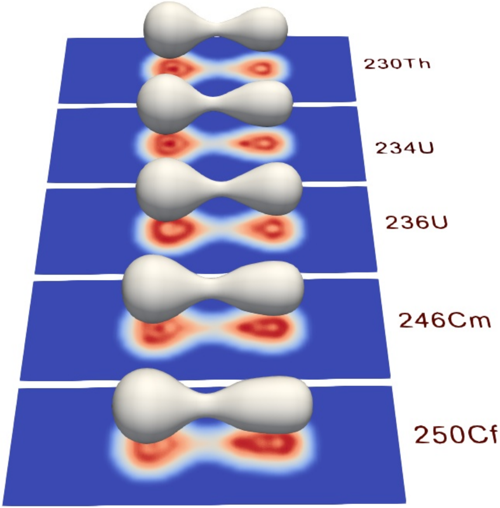

Other systems

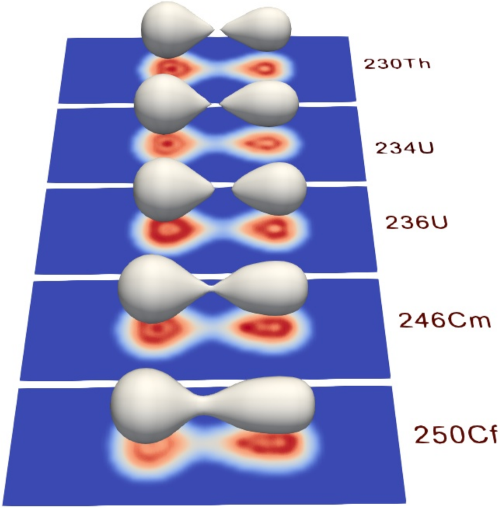

Other systems

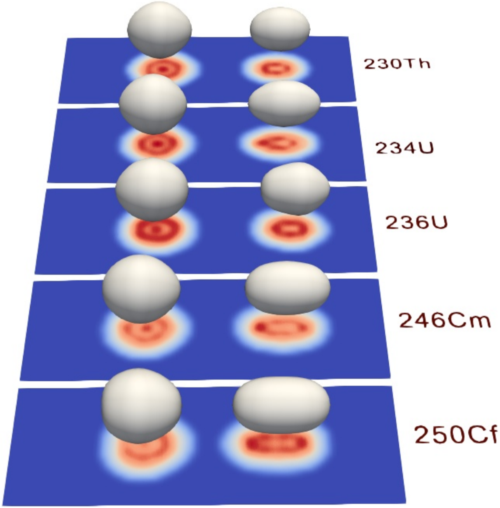

Other systems

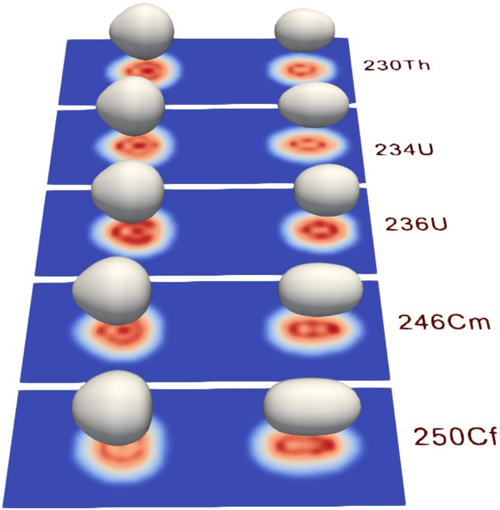

Why the fragments have octupole deformation ?

Similar effect on fusion reaction

^{40}Ca+^{40}Ca, $E3^- = 3.7$ MeV

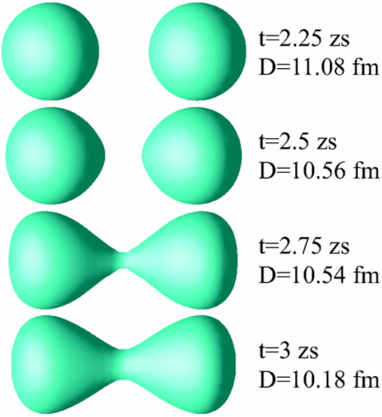

^{56}Ni+^{56}Ni, $E3^- = 7.5$ MeV

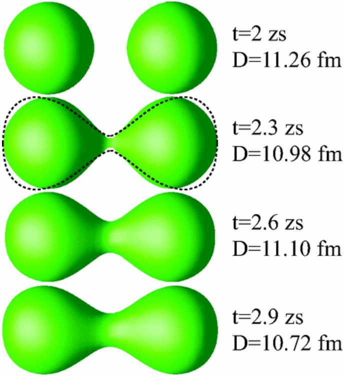

C. Simenel, M. Dasgupta, D. J. Hinde, and E. Williams, Phys. Rev. C 88, 064604 (2013).

Why the fragments have octupole deformation ?

Similar effect on fusion reaction

^{40}Ca+^{40}Ca, $E3^- = 3.7$ MeV

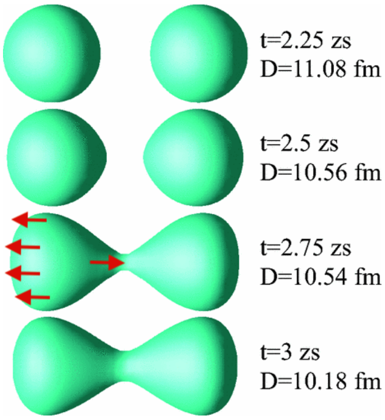

^{56}Ni+^{56}Ni, $E3^- = 7.5$ MeV

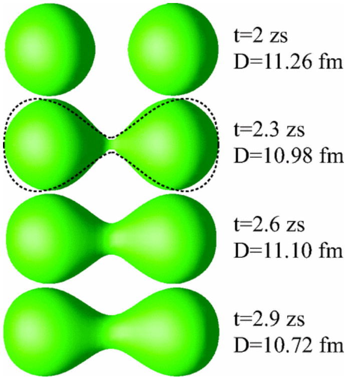

C. Simenel, M. Dasgupta, D. J. Hinde, and E. Williams, Phys. Rev. C 88, 064604 (2013).

Octupole deformation systematics

Skyrme Skm*.

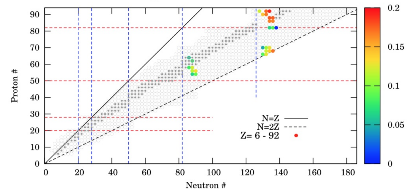

S. Ebata, and T. Nakatsukasa, Phys. Scr. 92 (2017) 064005

Gogny D1S

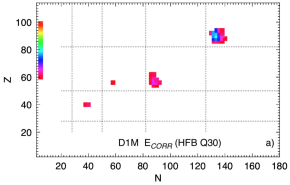

LM Robledo - J. phys. G : Nucl. and Particle Physics, 2015

Results from systematic calculation

In both calculations, the region $Z \simeq 54$, $N \simeq 88$ is favorable for octupole deformation .

Experimental results

^{144}Ba is found to be octupole in its groud state. Burcher et al. PRL 116 (2016).

Constraint HF+BCS octupole deformation with Sly4d

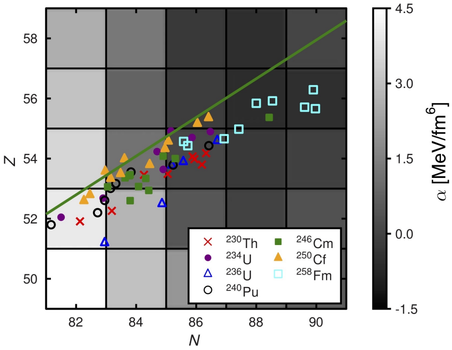

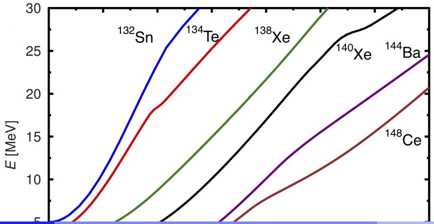

Structure, ^{144}Ba, Z=56, N=88

Q_2 - Q_3 potential energy surface

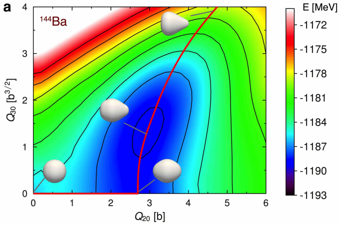

Single particle energy

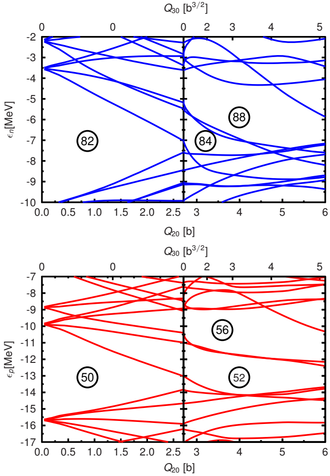

Structure

Single particle energies

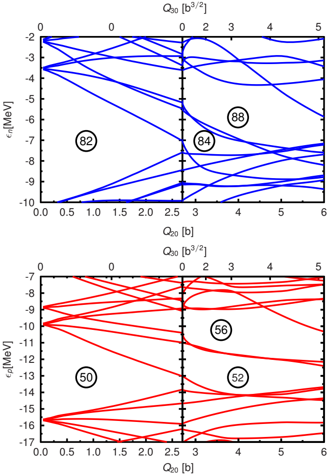

Experimental results

C. Böckstiegel et al. / Nuclear Physics A 802 (2008) 12–25

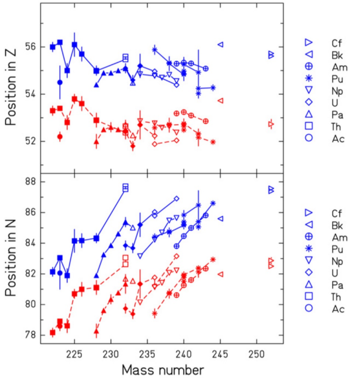

Deformation energy at the scission. Simple scission point model

$$E(N,Z) = E_{\beta_3=0.35}(N,Z) + E_{\beta_2=0.8}(N_{\rm tot}-N, Z_{\rm tot}-Z) + e^2\frac{Z(Z_{\rm tot}-Z)}{D_{sc}} \qquad (1)$$

With D_{sc}=17 fm. On the map, $E(N,Z)-E_{min}$ is shown.
For ^{240}Pu, $N_{\rm tot}$=146 and $Z_{\rm tot}$=94

Octupole deformation

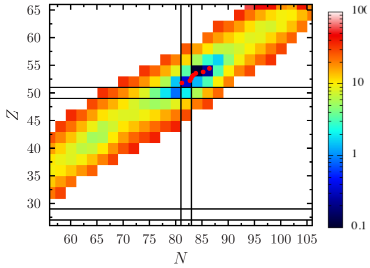

Spherical heavy fragment

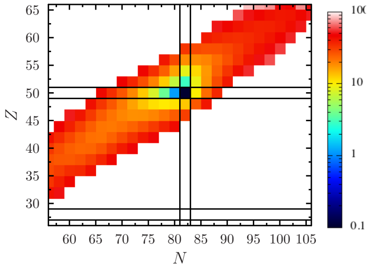

The energies have been calculated with the CHF+BCS theory Sly4d

Deformation energy at the scission. Simple scission point model

$$E(N,Z) = E_{\beta_3=0.35}(N,Z) + E_{\beta_2=0.8}(N_{\rm tot}-N, Z_{\rm tot}-Z) + e^2\frac{Z(Z_{\rm tot}-Z)}{D_{sc}} \qquad (1)$$

With D_{sc}=17 fm. On the map, $E(N,Z) - E_{min}$ is shown.
For ^{240}Pu, $N_{\rm tot}$=146 and $Z_{\rm tot}$=94

Octupole deformation

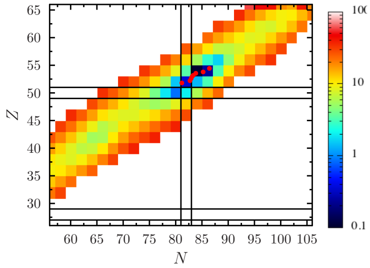

Experimental data

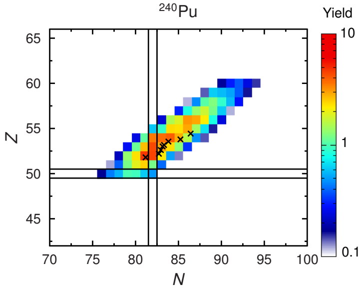

The energies have been calculated with the CHF+BCS theory Sly4d

Identification method with the nucleon localisation function

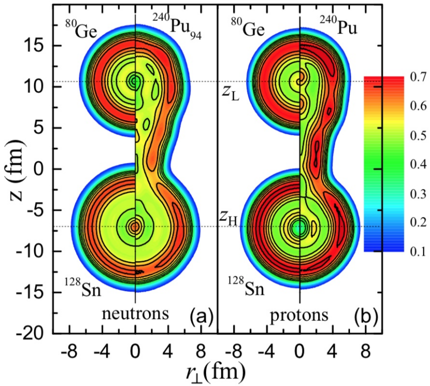

This method assumes that the pre-fragments have reflexion symmetry.

J. Sadhukhan, C. Zhang, W. Nazarewicz, and N. Schunck, PRC 96, 061301(R) (2017).

Identification with density

Technique of : M. Warda, A. Staszczak, and W. Nazarewicz, PRC 86, 024601 (2012).

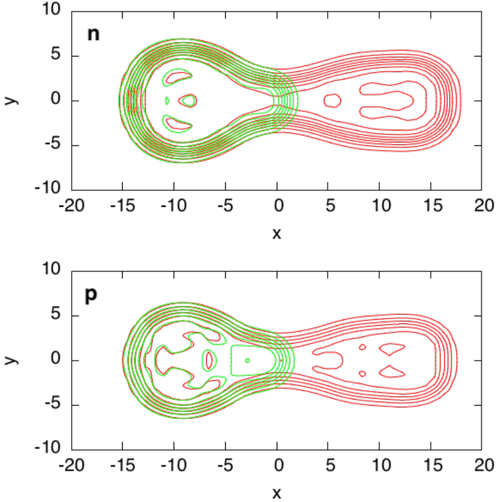

Green contour line : density of a ^{144}Ba with a constraint β_3=0.42
Red contour line : density of a fissioning ^{258}Fm (asymmetric mode)

Identification with nucleon localisation function

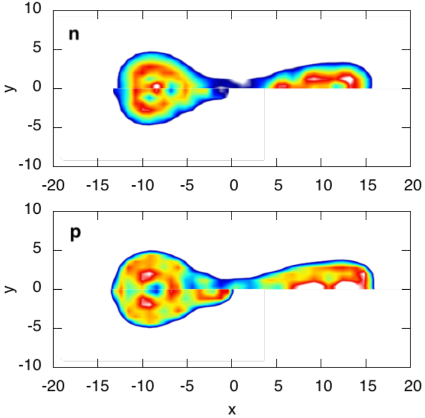

Top : NLF of a ^{144}Ba with a constraint β_3=0.42
Bottom : NLF of a fissioning ^{258}Fm (asymmetric mode)

Identification with nucleon localisation function

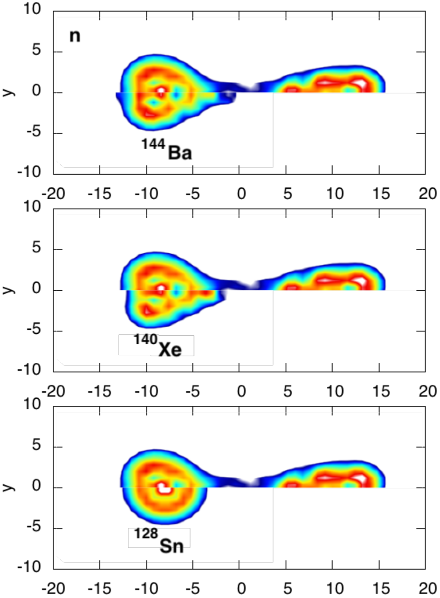

Identification method with octupole degree of freedom

Identification of the fragments as a function of time for the fission of ^{258}Fm

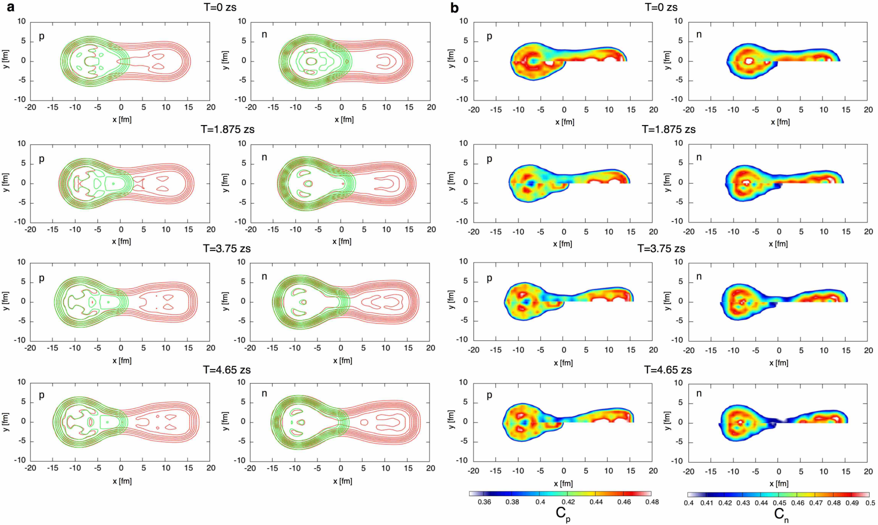

All of the systems are identified as ^{144}Ba with different β_3 values (resp. 0.14, 0.39, 0.39 and 0.42)

Identification method with octupole degree of freedom

Identification of the fragments at the scission for the different elements.

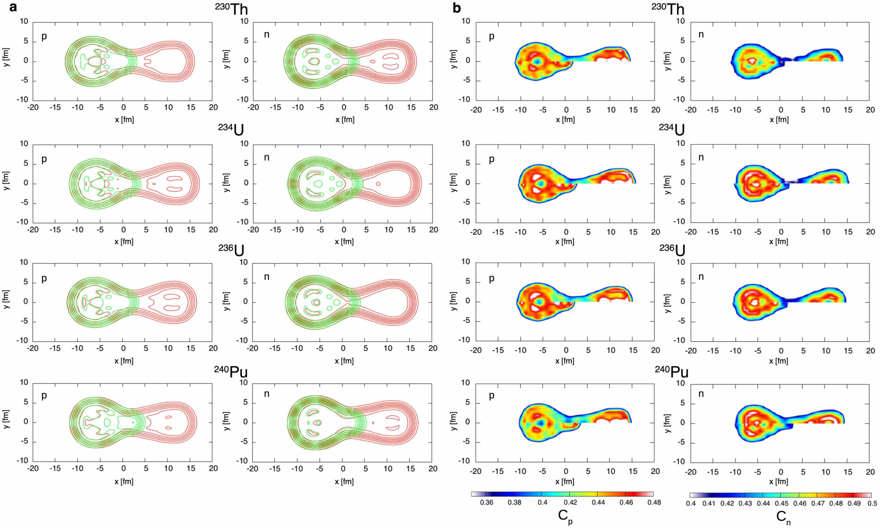

All systems are identified as ^{144}Ba with different β_3 values (resp. 0.28, 0.28, 0.27 and 0.44)

Conclusion

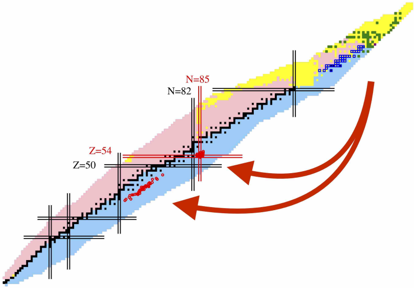

Mechanism

- The Nucleus-Nucleus interaction at the scission configuration favors the octupole shapes
- Shell structure favors octupole shape in the region Z $\simeq$ 52-56, N $\simeq$ 84-88
- Actinide fission fragments are driven in the region Z $\simeq$ 54, N $\simeq$ 86

G. Scamps, C. Simenel, arXiv :1804.03337 (2018).

Similar effect for other systems ?

J. Phys. G: Nucl. Part. Phys. **43** (2016) 073002 Topical Review

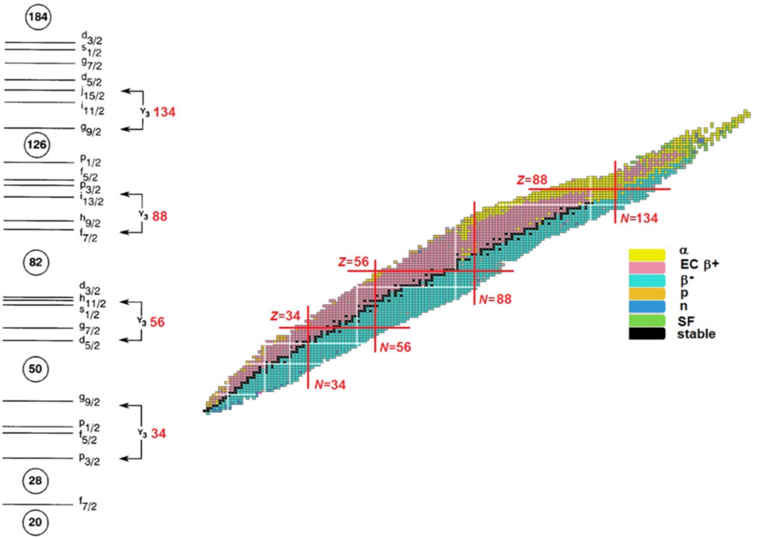

Experimental data of ^{180}Hg

A. N. Andreyev, et al., PRL 105, 252502 (2010)

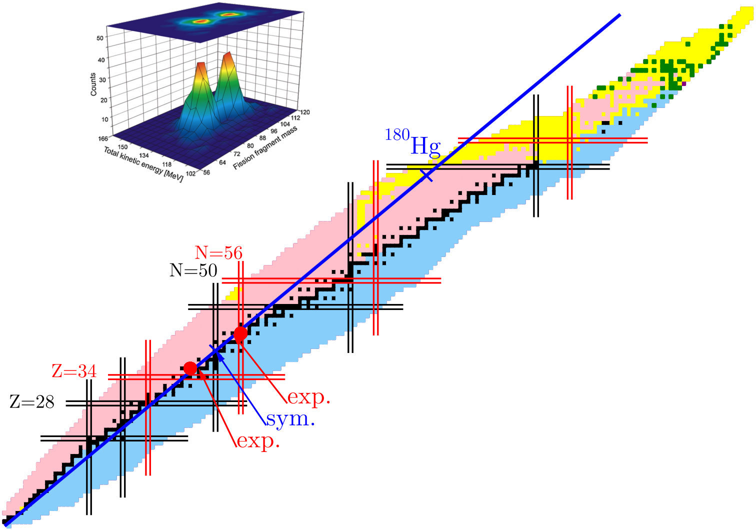

Experimental data of ^{178}Pt

I. Tsekhanovich, ArXiv :1804.01832

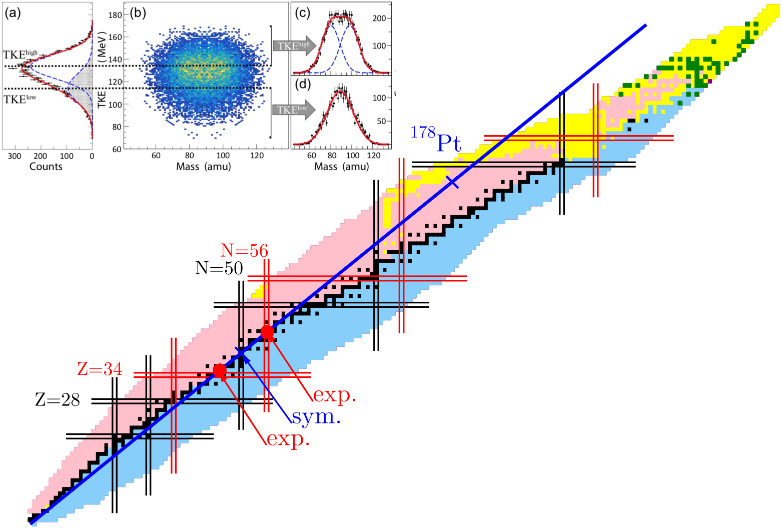

Similar effect of the octupole deformation ?

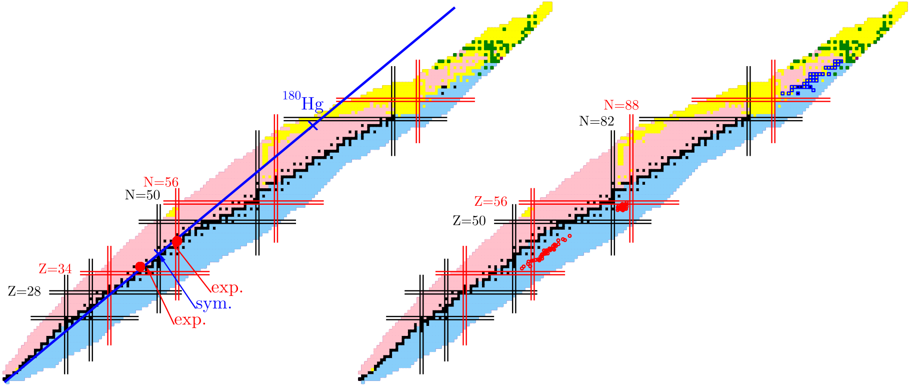

CHF+BCS calculation

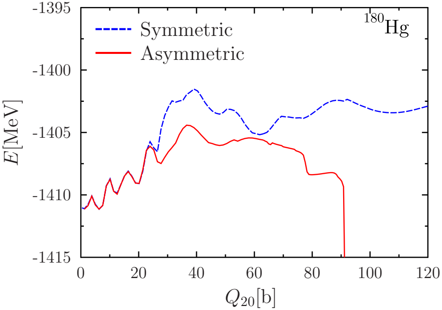

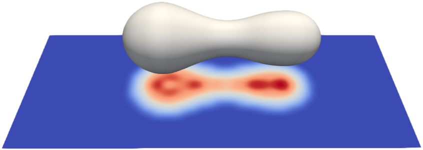

CHF+BCS calculations : Hg isotopic chain

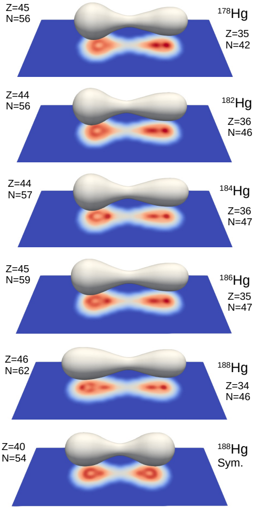

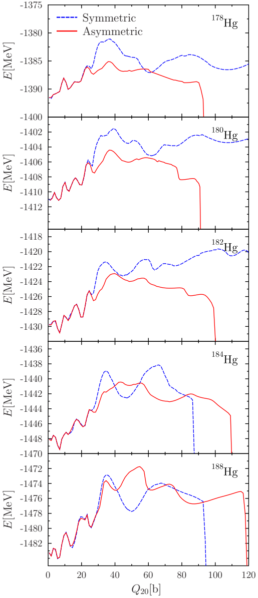

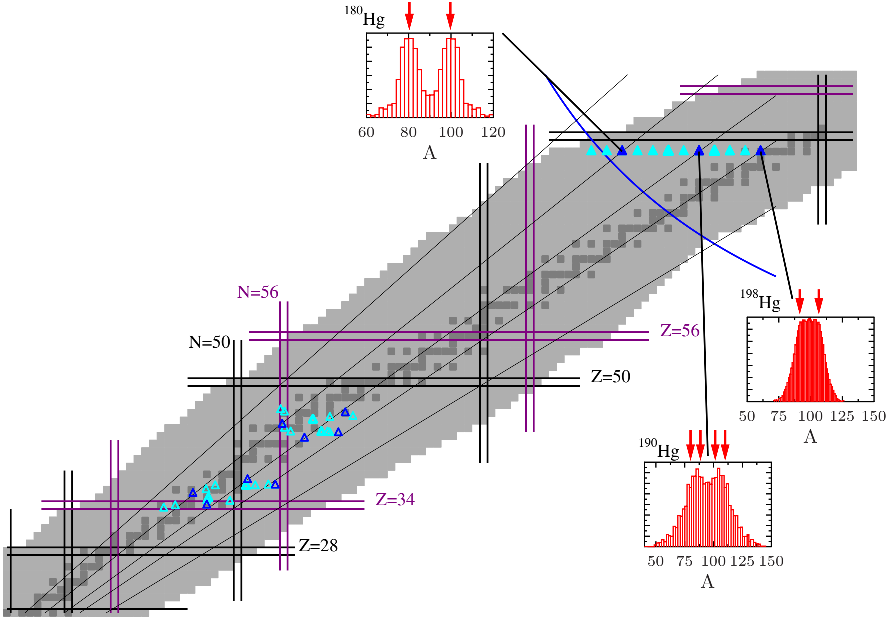

180Hg
60
80
100
120
A
198Hg
50
75
100
125
150
A
190Hg
50
75
100
125
150
A
N=56
N=50
Z=56
Z=50
Z=34
Z=28

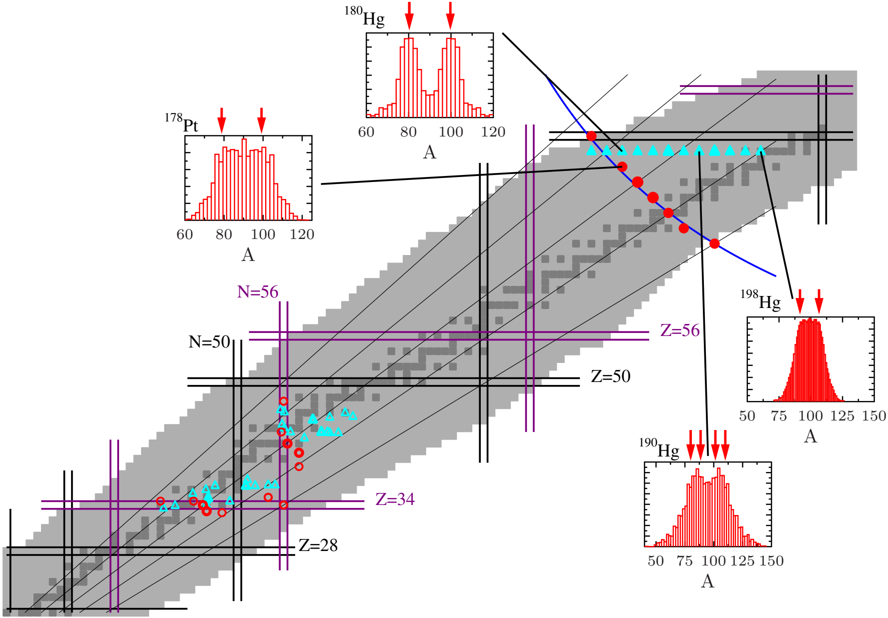

180Hg
60 80 100 120
A
178Pt
60 80 100 120
A
N=56
N=50
Z=56
Z=50
Z=34
Z=28
198Hg
50 75 100 125 150
A
190Hg
50 75 100 125 150
A

Deformation energy of the fragments

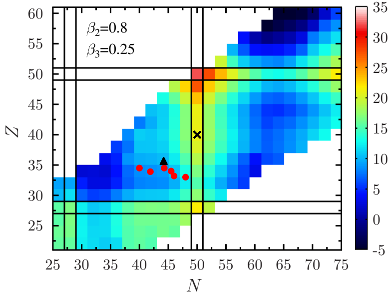

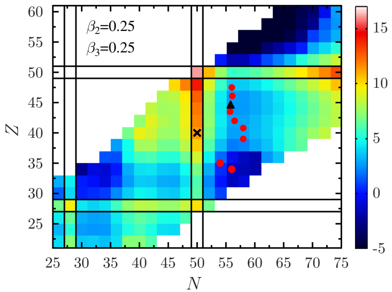

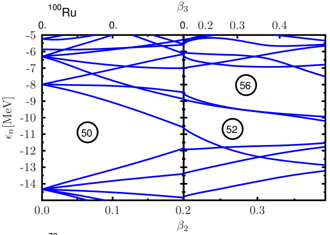

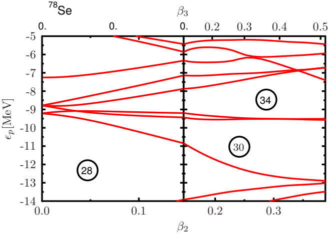

Conclusion

The fission process magnify the octupole shell structure

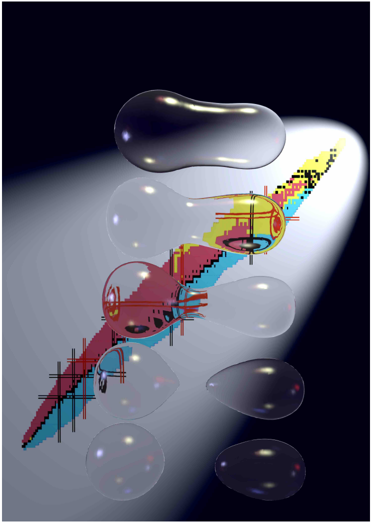

Preliminary Gogny-TDHFB calculation

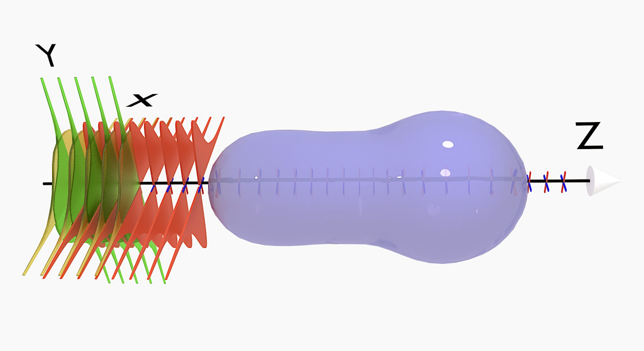

- x and y direction : Harmonic oscillator basis $n_x + n_y \leq N_{shell}$
- z direction : Cartesian mesh nz= 55

- $N_{\mathrm{base}} \simeq 3000$
- full cartesian mesh about 100 000 degrees of freedom

Y. Hashimoto

Preliminary test on ^{230}Th

TDHFB
(Gogny
D1S)

TDHF+BCS
(Sly4d)

Preliminary test on ^{230}Th

TDHFB
(Gogny
D1S)

TDHF+BCS
(Sly4d)

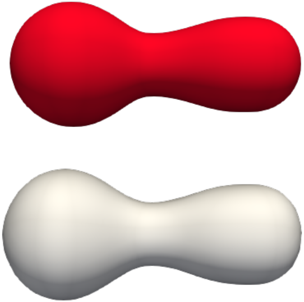

Preliminary test on ^{230}Th

TDHFB
(Gogny
D1S)

TDHF+BCS
(Sly4d)

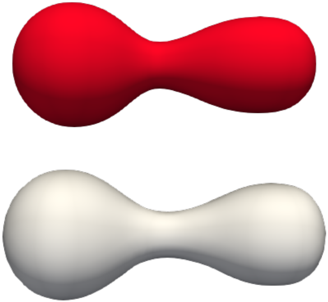

Preliminary test on ^{230}Th

TDHFB
(Gogny
D1S)

TDHF+BCS
(Sly4d)

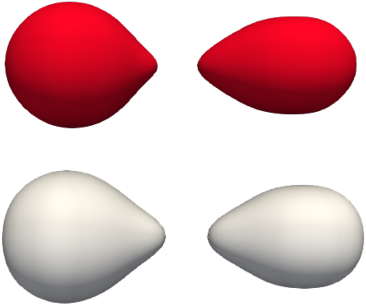

Preliminary test on ^{230}Th

TDHFB (Gogny D1S)

TDHF+BCS (Sly4d)

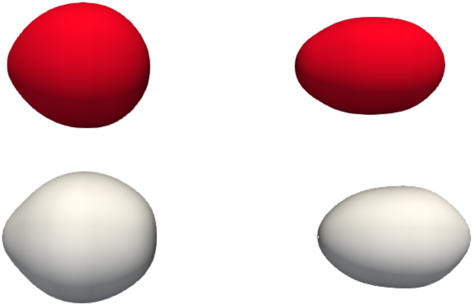

Outlook : Fission recycling

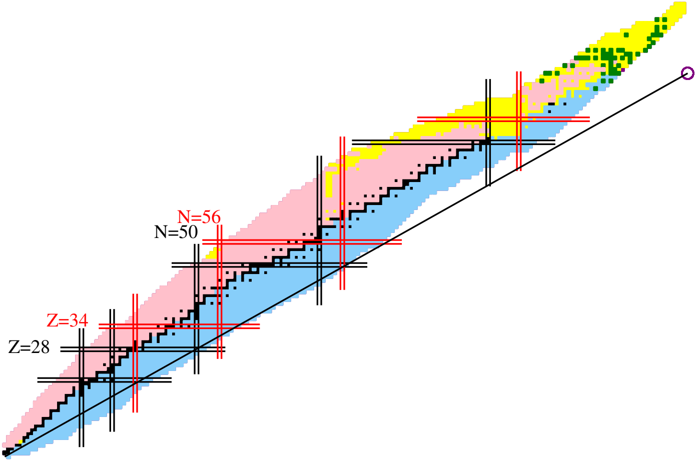

Region where BCS approximation is forbidden (due to continuum)

Thank you

Comparison TDHFB - TDHF+BCS

TDHF+BCS

- Based on TDHFB with the approximation : $\Delta_{ij} = \delta_{ij}\Delta_i$
- Evolution : $i\hbar \frac{d\varphi_i}{dt} = (\hat{h}_{MF} - \epsilon_i)\varphi_i$

$$i\hbar \frac{dn_i}{dt} = \Delta_i^* \kappa_i - \Delta_i \kappa_i^*$$

$$i\hbar \frac{d\kappa_i}{dt} = \kappa_i(\epsilon_i - \epsilon_{\bar{i}}) + \Delta_i(2n_i - 1)$$

Theoretical difference

- Numerical cost : TDHFB requires 1000 times more numerical resources
- Treatment of continuum states : BCS gas problem
- Continuity equation
- Number of pairing degrees of freedom (HFB $\Delta(r)$, BCS : $\Delta_{i\bar{i}}$)
- Spatial dependence of the pairing correlation

Comparison

A. Bulgac, P. Magierski, K. J. Roche, and I. Stetcu, PRL 116, 122504 (2016).

S no.	η	E^*	E_n	q_{zz}	q_{zzz}	t_{SS}	TKE^{syst}	TKE	A_L^{syst}	A_L	N_L^{syst}	N_L	Z_L^{syst}	Z_L
$S1$	0.75	8.05	1.52	1.78	−0.742	14 419	177.27	182	100.55	104.0	61.10	62.8	39.45	41.2
$S2$	0.5	7.91	1.38	1.78	−0.737	4360	177.32	183	100.56	106.3	60.78	64.0	39.78	42.3
$S3$	0	8.08	1.55	1.78	−0.737	14 010	177.26	180	100.55	105.5	60.69	63.6	39.81	41.9
$S4$	0	6.17	−0.36	2.05	−0.956	12 751	177.92	181		103.9		62.6		41.3

TABLE – TDHF+BCS results for ^{240}Pu

#	Q_0 [b]	E_0^*[MeV]	T_{fis} [fm/c]	Z_L	N_L	TKE [MeV]
1	45.4	1.46	6480	40.21	60.77	171.5
2	46.7	0.8	4830	40.83	62.68	181.8
3	50.5	-1.16	26970	42.2	64.83	181.8
4	53.0	-2.13	6750	41.39	63.05	177.9
5	56.8	-3.5	4800	40.99	62.85	177.2
6	59.3	-4.3	5400	40.45	62.17	178.4
7	63.1	-5.31	6630	39.55	59.58	162.7
8	71.9	-7.8	1020	41.8	63.28	179.9